

Reconnection-driven plasmoids in blazars: fast flares on a slow envelope

Dimitrios Giannios^{1,2*}

¹*Department of Physics, Purdue University, 525 Northwestern Avenue, West Lafayette, IN 47907, USA*

²*Max Planck Institute for Astrophysics, Box 1317, D-85741 Garching, Germany*

Received / Accepted

ABSTRACT

TeV flares of duration of ~ 10 minutes have been observed in several blazars. The fast flaring requires compact regions in the jet that boost their emission towards the observer at an extreme Doppler factor of $\delta_{\text{em}} \gtrsim 50$. For ~ 100 GeV photons to avoid annihilation in the broad line region of PKS 1222+216, the flares must come from large (pc) scales challenging most models proposed to explain them. Here I elaborate on the magnetic reconnection minijet model for the blazar flaring, focusing on the inherently time-dependent aspects of the process of magnetic reconnection. I argue that, for the physical conditions prevailing in blazar jets, the reconnection layer fragments leading to the formation a large number of plasmoids. Occasionally a plasmoid grows to become a large, “monster” plasmoid. I show that radiation emitted from the reconnection event can account for the observed “envelope” of \sim day-long blazar activity while radiation from monster plasmoids can power the fastest TeV flares. The model is applied to several blazars with observed fast flaring. The inferred distance of the dissipation zone from the black hole and the typical size of the reconnection regions are $R_{\text{diss}} \sim 0.3 - 1$ pc and $l' \lesssim 10^{16}$ cm, respectively. The required magnetization of the jet at this distance is modest: $\sigma \sim$ a few. Such distance R_{diss} and reconnection size l' are expected if the jet contains field structures with size of the order of the black-hole horizon.

Key words: galaxies: active – BL Lacertae objects: individual: PKS 2155–304 – BL Lacertae objects: individual: PKS 1222+216 – gamma rays: theory.

1 INTRODUCTION

Blazars are extremely bright and fast varying extragalactic sources observed throughout the electromagnetic spectrum. Depending on the presence or absence of observed optical emission lines they are classified as Flat Spectrum Radio Quasars (FSRQs) or BL Lac objects, respectively (Urry & Padovani 1995). In either case, it is believed that the blazar emission is powered by relativistic jets which emerge from supermassive black holes and beam their emission at our line of sight.

Blazar variability on timescales ranging from hours to decades has been commonly observed at various wavelengths of the electromagnetic spectrum (see, e.g., Böttcher 2007). The recent discovery of blazar flaring on $\sim 5 - 10$ minute timescales came as great surprise. Such extreme flaring has now been observed from several objects both BL-Lacs and FSRQs [Markarian 421 (Gaidos et al. 1996); PKS 2155–304 (Aharonian et al. 2007; hereafter referred to as PKS 2155), Markarian 501 (Albert et al. 2007; Mrk 501), and the prototype object of the class BL Lac (Arlen et al. 2013); and the FSRQ source PKS 1222+216 (Aleksić et al. 2011; hereafter PKS

1222)]. Fast-evolving TeV flares are, therefore, a generic feature of blazar activity.

Ultra-fast flares pose several challenges to theoretical models for the blazar emission. The observed timescale of variability is too short to originate directly from the central engine. Modulations of the properties of the plasma in the vicinity of the black hole are limited by causality arguments to be longer than the light crossing time of the horizon $t_v \gtrsim R_{\text{Sch}}/c \simeq 10^4 M_9$ sec, where $R_{\text{Sch}} = 2GM_{\text{BH}}/c^2$ and $M_{\text{BH}} = 10^9 M_9 M_\odot$. The observed ~ 10 -min-long flares are far more likely to originate from compact emitting regions that somehow form in the jet (Begelman et al. 2008; Giannios et al. 2009; Narayan & Piran 2012). Furthermore, for the TeV photons to escape the source in PKS 2155 and Mrk 501 the emitting blob must have a Doppler boosting of $\delta \gtrsim 50 - 100$ towards the observer (Begelman et al. 2008; Finke et al. 2008; Mastichiadis & Moraitis 2008). This is much larger than the Lorentz factor $\Gamma_j \sim 10 - 20$ typically inferred for blazar jets from superluminal motions (see, e.g., Savolainen et al. 2010). Moreover, the γ -ray flaring from PKS 1222 directly constrains the location of the emitting region. For $\gtrsim 100$ GeV photons to escape the *observed* broad line region of the FSRQ, the emitting region must be located at scales $\gtrsim 0.5$ pc (Tavecchio et al. 2011; Nalewajko et al. 2012). This constraint is practically inde-

* E-mail: dgiannio@purdue.edu (DG)

pendent of the assumed geometry of the broad-line region (Tavecchio & Ghisellini 2012). Given the large dissipation distance and the large inferred energy density at the source, the intense flaring from PKS 1222 implies an unrealistically large jet power unless the emitting material is, again, strongly boosting its emission with $\delta \gtrsim 50$ (Nalewajko et al. 2012)¹. One final clue for the origin of the fast flaring is that it is observed on top of an envelope of longer \sim day-long flares. During the fast flaring the flux increases by a factor of \sim a few with respect that of the envelope (Aharonian et al. 2007; Albert et al. 2007).

A large number of theoretical interpretations have been put forward to explain the fast flares in *individual* sources. Fast beams of particles at the light cylinder (Ghisellini & Tavecchio 2008) or the interaction of the jet with a red giant star (Barkov et al. 2012) are some of them. Rarefaction waves in magnetized shells (Lyutikov & Lister 2010), relativistic turbulence in the jet (Narayan & Piran 2012) or reconnection-driven minijets (Giannios et al. 2009) may also be responsible for the fast flares. I focus here on the latter possibility.

In the MHD jet paradigm (Blandford & Payne 1982) the jet is expected to emerge from the central engine in the form of a Poynting-flux dominated flow. If the magnetic field configuration is appropriate after the jet acceleration and collimation phases, magnetic reconnection can effectively dissipate magnetic energy in the flow. As pointed out in Giannios et al. (2009; 2010; Nalewajko et al. 2011) magnetic reconnection dissipates energy in compact regions characterized by fast motions within the jet, i.e., the radiating plasma can move faster than the jet material on average. The extreme Doppler boosting of the emitting region and its small size can naturally account for the fast-evolving flares observed in blazars.

The reconnection minijet model is, however, based on a *steady* reconnection picture. Both observations and recent advances in reconnection theory reveal that reconnection is a highly time-dependent and dynamical process. Time dependent aspects of reconnection turn out to be critical in understanding the multiple observed timescales related to blazar flaring. The goal of this work it twofold: (i) to relax the steady-state assumptions of the reconnection model for blazar flaring and (ii) confront the model against all the available observational constraints.

In the Sec. 2 I summarize some of the recent observational and theoretical progress in understanding time-dependent aspects of magnetic reconnection. In Sec. 3 this knowledge is applied to a blazar jets predicting the relevant timescales and energetics of flaring. The model is applied to specific sources in Sec. 4. I conclude in Sec. 5.

2 MAGNETIC RECONNECTION: A DYNAMICAL PROCESS

In this Section I summarize recent progress in magnetic reconnection theory that is relevant to the blazar jet application presented here. Reconnection is the process of fast release of magnetic energy during a topological rearrangement of magnetic field lines. It takes place when magnetic field lines of opposite polarity are coming together towards the reconnection plane ($x - y$ plane in fig. 1) and annihilate, liberating magnetic energy that heats the plasma and accelerates particles. The large scale l of the reconnection region is

determined by the distance over which the magnetic field strength drops by a factor of ~ 2 (along the y direction). The magnetic pressure gradient and also magnetic tension along the y direction result in the bulk acceleration of the reconnected material to the Alfvén speed V_A of the upstream fluid. The fast outflow in the downstream allows for fresh magnetized fluid to enter the region and reconnect.

Observationally reconnection has been extensively studied during solar flares and in Earth’s magnetotail. Laboratory experiments complement these studies in a controlled environment. A richness of processes that take place on very different timescales have been revealed by these works (see, e.g., Aschwanden 2002). A characteristic long timescale of the process is the global reconnection timescale $t_{\text{rec}} \sim l/\epsilon V_A$ over which the magnetic energy stored in a region of typical scale² l is released. Here ϵ parametrizes the reconnection speed; with $\epsilon \sim 0.1$ been a typical observationally inferred value. *Besides the global reconnection timescale, much shorter timescale variability and eruptive events are evident both observationally and experimentally highlighting the very dynamical nature of the process* (see e.g., Lin et al. 2005; Park et al. 2006; Karlický & Kliem 2010). For instance a solar flare of typical duration of ~ 10 min can show strong variability on \sim s timescale (see, e.g., Karlický & Kliem 2010).

For some time the reconnection theory has been dominated by steady-state models (Sweet 1958; Parker 1957, Petschek 1964). They provide intuition on how *average* properties such as the reconnection speed, the outflow speed and temperature of the reconnected fluid depend on parameters. Steady state models assume a continuous inflow of plasma in the reconnection region and a smooth outflow. As such they cannot account for the erratic behavior observed at the current sheet.

A distinctly different picture has emerged from recent theoretical studies of magnetic reconnection. When the resistivity η is sufficiently low, e.g., the corresponding Lundquist number $S = V_A l / \eta \gg S_c = 10^4$ (as expected in most Astrophysical environments) the reconnection current sheet is formally predicted by the Sweet-Parker theory to be extremely thin, with thickness $\delta/l = S^{-1/2} \ll S_c^{-1/2} \sim 0.01$. Very thin current sheets suffer from tearing instabilities that lead to their fragmentation to a large number of plasmoids separated by smaller current sheets (Loureiro et al. 2007; Lapenta 2008; Daughton et al. 2009; Loureiro et al. 2009; Samtaney et al. 2009; Bhattacharjee et al. 2009; Loureiro et al. 2012b). As a result the reconnection process is fast and resistivity-independent. Plasmoids grow fast through mergers and leave the reconnection at a speed comparable to the Alfvén speed of the upstream plasma (Uzdensky et al. 2010; Loureiro et al. 2012a). The typical plasmoid forms away from the reconnection center (the, so-called x-point) at $y \sim l$ and grows up to a characteristic size $R_p \ll l$. Plasmoids that form fairly close to the reconnection center have, however, more time available to merge and grow on their way out of the reconnection region. These plasmoids undergo significant (exponential) growth to reach macroscopic scale. They are referred to as “monster” plasmoids (Uzdensky et al. 2010). Their size reaches a scale $R_p \approx S_c^{-1/4} l \equiv fl \approx 0.1l$, i.e., approaching the global reconnection scale. The growth of the size of a plasmoid is exponential $\propto e^{t/t_A}$, where $t_A = l/V_A$. The mass doubling of the plasmoid takes place on a timescale $\sim t_A$ with the plasmoid emerging from the reconnection region at the Alfvén speed V_A . Resistive MHD simu-

¹ For PKS 1222 a lower $\delta \sim 20$ is allowed *if* the distribution of energetic particles is extremely focused in the rest frame of the emitting material; see Nalewajko et al. (2012).

² For simplicity and throughout this paper I will assume that the reconnection region has the same characteristic scale l in all directions.

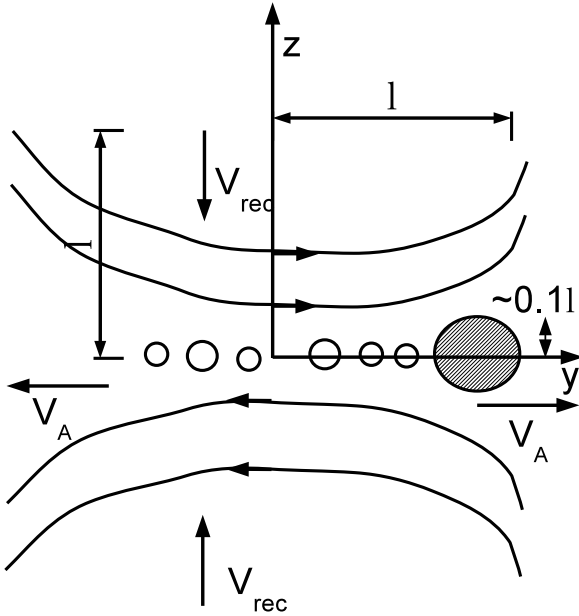


Figure 1. Sketch of the magnetic reconnection region with a large scale l . Magnetic field lines of opposite polarity annihilate at the $x - y$ plane with speed v_{rec} , i.e., the reconnection proceeds on a global timescale $t_{\text{rec}} = l/\epsilon c$. The physical conditions relevant to AGN jets, the current layer is expected to fragment to a large number of sub-layers separated by plasmoids (Loureiro et al. 2007). The plasmoids leave the reconnection region with the Alfvén speed V_A powering the “envelope” emission. Occasionally, plasmoids grow to become “monster” plasmoids (shaded blob) with scale $fl \sim 0.1l$ giving rise to powerful, fast-evolving flares of duration $t_{\text{flare}} \ll t_{\text{rec}}$.

lations support this theoretical picture (see, e.g., Bhattacharjee et al. 2009; Loureiro et al. 2012a).

The monster plasmoids consist of energetic particles that have undergone acceleration in the secondary current sheets. Additional acceleration of particles takes place during the merging process of the plasmoids (Zenitani & Hoshino 2001; 2005; Drake et al. 2006, Sironi & Spitkovsky 2011; although the energy spectrum of the particles depends on the details and is still topic of investigation). As I demonstrate below, the macroscopic scale of the monster plasmoids, their short growth timescale, and fast motion and energetic particles that they contain make them natural candidates for powering the ultra-fast blazar flares.

3 APPLICATION TO BLAZAR FLARING

In the MHD-driving paradigm for jets (e.g., Blandford & Payne 1982), it is postulated that jets emerge from the central engine in the form of Poynting-flux dominated flows. Further out the flow converts part of its magnetic energy into kinetic. At a (both theoret-

ically and observationally very uncertain) distance R_{diss} , the blazar emission emerges. If the magnetic field configuration is appropriate, magnetic reconnection can effectively dissipate magnetic energy in the flow and power the blazar emission. I assume that substantial magnetic energy release takes place in reconnection regions of characteristic scale l .³ The magnetization $\sigma \equiv B^2/4\pi\rho c^2$ of the jet at the dissipation region is assumed to be $\sigma \gtrsim 1$. As a result, the Alfvén four velocity and, correspondingly, that of the reconnection outflows is expected to be moderately relativistic $u_{\text{out}} \simeq u_A = \sqrt{\sigma}$ (Lyubarsky 2005).

The location of R_{diss} and the scale l are highly model dependent. The trigger of magnetic dissipation may be instabilities that develop in the jet. Even if the jet is launched by an axisymmetric magnetic field configuration, non-axisymmetric instabilities can introduce smaller scale field structures. Current-Driven Instabilities (CDIs) are likely to be the most relevant in strongly magnetized jets (Eichler 1993; Begelman 1998; Giannios & Spruit 2006). The observational indications that the jet opening angle is related to the jet Lorentz factor through the relation $\theta_j \Gamma_j \sim 0.2$ (Pushkarev et al. 2009) implies that causal contact is established in the transverse direction of a high- σ jet. Under these conditions, CDIs can potentially grow as soon as the jet develops a dominant toroidal field component. CDIs are non-axisymmetric instabilities that reorganize the field configuration. In the non-linear stages of their development small scale field reversals may be induced in the jet allowing for energy extraction through reconnection (Moll 2009). The non-linear stages of CDIs are, however, poorly understood making it hard to predict the distance at which they develop or the characteristic scales of the reconnection layers.

An interesting alternative is that the magnetic field is not axisymmetric at the launching region. The jet contains, instead, small-scale field structures imprinted from the central engine (Romanova & Lovelace 1997, Levinson & van Putten 1997, Giannios 2010, McKinney & Uzdensky 2012). Such configurations can introduce field reversals in the jet of the order of the size of the black hole horizon $R_{\text{sch}} = 3 \times 10^{14} M_9$ cm (in the lab frame). The scale of the field reversal in the rest frame of the jet is $l' \simeq \Gamma_j R_{\text{sch}} \simeq 6 \times 10^{15} \Gamma_{j,20} M_9$ cm. In such configuration, substantial dissipation takes place when the reconnection timescale $t_{\text{rec}} = l'/\epsilon c = \Gamma_j R_{\text{sch}}/\epsilon c$ becomes comparable to the expansion timescale of the jet $t_{\text{exp}} = R_{\text{diss}}/\Gamma_j c$, i.e., at a distance

$$R_{\text{diss}} \simeq \Gamma_j^2 R_{\text{sch}}/\epsilon = 1.2 \times 10^{18} M_9 \Gamma_{j,20}^2 \epsilon_{-1}^{-1} \text{ cm.} \quad (1)$$

In the following, and for more concrete estimates, I adopt R_{diss} given by eq. (1) and $l' = \Gamma_j R_{\text{sch}}$ as motivated by the proceeding discussion. The model presented here can, however, be applied to any choice of the parameters R_{diss} and l' .

3.1 Fast flares from monster plasmoids

For the physical conditions prevailing at the reconnection region relevant to AGN jets, the current sheet is expected to fragment into a large number of plasmoids while the reconnection process proceeds fast (see Appendix A for details). Some plasmoids regularly grow into “monster” plasmoids, i.e., large magnetized blobs that contain energetic particles freshly injected by the reconnection process (Uzdensky et al. 2010). The relativistic motion of the plasmoids in the rest frame of the jet results in additional beaming of

³ Hereafter primed quantities are measured in the rest frame of the jet while double-primed quantities in the rest frame of a plasmoid.

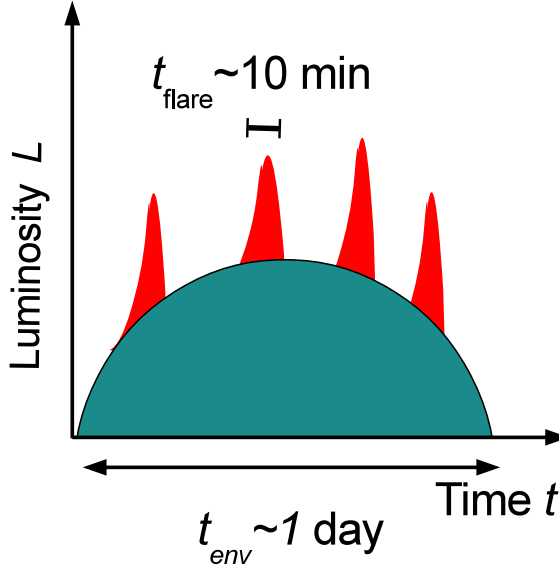


Figure 2. Sketch of the envelope-flare structure of the emission from a reconnection layer. The envelope duration corresponds to that of the reconnection event: $t_{\text{env}} = l'/\Gamma_j c$. Monster plasmoids power fast flares which show exponential rise and last for $t_{\text{flare}} = 0.1l'/\delta_p c$. For an envelope of ~ 1 day blazar flaring the model predicts that monster plasmoids result in ~ 10 -minute flares.

their emission (i.e., beyond that induced by the jet motion). When the layer's orientation is such that plasmoids beam their emission towards the observer, powerful and fast evolving flares emerge. *Here we focus on the characteristic observed timescales and luminosities resulting from plasmoids that form in the reconnection region.* To this end I assume that the dissipated energy is efficiently converted into radiation. In practice electrons are likely to be responsible for the emission (e.g. see Nalewajko et al. 2012) so I, in effect, assume that a significant amount of the dissipated energy is deposited to electrons which undergo fast radiative cooling. The latter assumption will be checked a posteriori. The former maybe justified by the efficient electron acceleration by the electric field present at the current sheets but remains an assertion. This study can be trivially generalized by including the efficiency factor with which dissipated energy converts into radiation.

Consider a spherical blob (or plasmoid) emerging from the reconnection layer moving with the Alfvén speed of the reconnection upstream ($V_A = \sqrt{\sigma/(1+\sigma)}c$), i.e. with a corresponding bulk Lorentz factor $\gamma_p = \sqrt{1+\sigma} \sim$ a few (measured in the jet rest frame) and of size $R_p'' = fl'$.⁴ The growth of the plasmoid in

⁴ I treat the plasmoid as a sphere in its own rest frame (and not in the jet rest frame). It is unclear which approximation describes better the reconnection

the reconnection layer is exponential with time. The observed rise time for the plasmoid emission is $t_{\text{rise,obs}} \approx R_p''/\delta_p c$, where δ_p is the Doppler boost of the plasmoid radiation towards the observer. The plasmoid subsequently cools down and expands on a similar observed timescale $t_{\text{decline,obs}} \sim R_p''/c\delta_p$. We, therefore, define as the variability timescale $t_v \equiv t_{\text{rise,obs}} = fl'/c\delta_p$. For field reversals imprinted from the central engine $l' \approx \Gamma_j R_{\text{Sch}}$ resulting in

$$t_v = \frac{f\Gamma_j R_{\text{Sch}}}{\delta_p c} = 400f_{-1}\Gamma_{j,20}M_9\delta_{p,50}^{-1} \text{ s}, \quad (2)$$

where $\delta_p = 50\delta_{p,50}$, $f = 0.1f_{-1}$, $\Gamma_j = 20\Gamma_{j,20}$. Flaring on several minute timescale is therefore expected in this picture.

Consider a jet emerging from a supermassive black hole with (isotropic equivalent) power L_{iso} , opening angle θ_j and Lorentz factor Γ_j . We also assume that $\theta_j\Gamma_j = 0.2$ as indicated by observations (Pushkarev et al. 2009). The typical bulk Lorentz factor of gamma-ray active blazars is $\Gamma_j \sim 10 - 20$ (Savolainen et al. 2010; Piner et al. 2012). The energy density at the dissipation, or “blazar”, zone is

$$U_j' = \frac{L_{\text{iso}}}{4\pi(\theta_j R_{\text{diss}})^2 \delta_j^4 c} = 0.12 \frac{L_{\text{iso},48} \epsilon_{-1}^2}{M_9^2 \Gamma_{j,20}^2 \delta_{j,20}^4} \text{ erg/cm}^3, \quad (3)$$

where the L_{iso} is normalized to 10^{48} erg/s and the dissipation distance is given by eq (1).

Pressure balance across the reconnection layer requires the energy density of the plasmoid to be similar to that of the jet $U_p'' \sim U_j'^5$. Assuming efficient conversion of dissipated energy into radiation (assumption to be verified in Sect. 4.3), the rest-frame luminosity of the plasmoid is thus $L'' = U_p'' 4\pi R_p''^2 c$. This luminosity can be converted to the observed luminosity $L_{\text{p,obs}} = \delta_p^4 L''$. Because of the $R_p''^2$ dependence of the luminosity it is clear that the largest “monster” plasmoids (with $R_p'' = fl'$, $f \approx 0.1$) power the brightest flares. Putting everything together, the observed luminosity of the plasmoid is

$$L_{\text{p,obs}} = 10^{47} \frac{\epsilon_{-1}^2 f_{-1}^2 \delta_{p,50}^4 L_{\text{iso},48}}{\delta_{j,20}^4} \text{ erg/s}. \quad (4)$$

The Doppler factor of the plasmoid δ_p depends on several parameters. It is related to Γ_j , γ_p , the angle of the plasmoid with respect to the jet motion and the observer's angle of sight. For perfectly aligned jet, plasmoid and observer $\delta_p \approx 4\Gamma_j\gamma_p$. In, perhaps, more common situations where the reconnection layer is at a large $\theta \sim \pi/2$ angle with respect to the jet propagation (as seen in the jet rest) and fairly aligned with the observer (giving powerful flares) $\delta_p \sim \Gamma_j\gamma_p$. For the demonstrative arithmetic examples used here we adopt $\delta_p = 1.25\Gamma_j\gamma_p = 50\Gamma_{j,20}\gamma_{p,2}$. One can see (see eq. 2) that powerful flares on a timescale of ~ 10 min is possible even with very modest relativistic motions within the jet⁶ $\gamma_p \sim 2$.

plasmoids for relativistic reconnection. In the limit of modest relativistic motions of interest here ($\gamma_p \sim$ a few), this distinction is not affecting the results presented here by much.

⁵ The exact relation of U_p'' and U_j' depends on the magnetic and heat content of the upstream and the plasmoid. For instance balancing the pressure of cold, strongly magnetized upstream $p_j = B^2/8\pi = U_j'/2$ with that of an assumed relativistically hot plasmoid $p_p = U_p''/4$, we find $U_p'' = 2U_j'$. The expression is slightly different if the magnetic field contributes to the pressure of the plasmoid. The Assumption $U_p'' \sim U_j'$ is expected to hold within a factor of ~ 2 independently of these details.

⁶ Narayan & Piran (2012) come to a different conclusion concerning the fastest flares expected by magnetic reconnection. Their analysis assumes steady reconnection and is therefore applicable to the global reconnection

3.1.1 Ejection of multiple monster plasmoids

During a reconnection event multiple monster plasmoids are expected to form. The seed of a monster plasmoid forms fairly close to the reconnection center region $y \ll l'$ and spends sufficient time in the reconnection region to grow to a large size. 2D simulations (Loureiro et al. 2012a) indicate that monster plasmoids form every a few Alfvén times t_A or at a rate of $\sim 0.3t_A^{-1}$. It appears likely that 2D simulations underestimate the rate of formation of monster plasmoids. The actual rate may be higher when the 3D structure of the layer is considered. The x-point is in reality an elongated structure (along the x-axis of fig. 1) providing a larger physical region where the seeds of monster plasmoids form. Monster plasmoids potentially form at a rate up to $l'/R'_p \sim 10$ higher than that found in 2D studies. Clearly this question can only be answered high resolution, 3D resistive MHD simulations. If monster plasmoids emerge at a rate $\sim (0.3-3)t_A^{-1}$, some $(3-30)/\epsilon_{-1}$ plasmoids are expected from a single reconnection layer powering multiple flares. The observed properties of the monster plasmoids are determined by the basic properties of the reconnection region that generates them. To the extent that all monster plasmoids reach similar size of $\sim 0.1l'$, the model predicts a similar duration and brightness for this sequence of fast flares. Smaller plasmoids $f < 0.1$ can power even faster flares since $t_v \propto f$ albeit of lower peak luminosity ($L_p \propto f^2$). A sketch of such pattern is shown in Fig. (2).

3.2 The “envelope emission” from the reconnection region

The bulk motion of a monster plasmoid is expected to be similar to the speed of other structures (e.g. smaller plasmoids) leaving the reconnection region. When the plasmoid emission is beamed towards the observer (powering a fast flare), the overall emission from the current layer is also beamed by a similar factor. The emission from the layer forms a slower-evolving envelope. In the following I calculate the timescale and luminosity of the emission from the reconnection layer.

At the dissipation distance R_{diss} , the reconnection proceeds within the expansion time of the jet which is observed to last for $t_{\text{exp,obs}} \simeq R_{\text{diss}}/\Gamma_j^2 c$. Therefore, $t_{\text{exp,obs}}$ corresponds to the observed duration of the envelope emission (using also eq. (1)):

$$t_{\text{env}} = \frac{R_{\text{diss}}}{\Gamma_j^2 c} = 10^5 \frac{M_9}{\epsilon_{-1}} \text{ s.} \quad (5)$$

The duration of the envelope emission is \sim days. Such timescale is characteristic of blazar flares (See next Section).

The (lab frame) energy available to power the envelope emission is $E_{\text{env}} = U_j 2l'^3/\Gamma_j$, where $U_j = \Gamma_j^2 U'_j$ is the energy density of the jet and $2l'^3/\Gamma_j$ accounts for (lab frame) volume of the reconnection region that powers each minijet (see fig. 1). The emitted luminosity of the reconnection region is $E_{\text{env}}/t_{\text{env}}$. It can be converted into *observed* luminosity by accounting for beaming factor of the emission $\sim \delta_p^2$:

$$L_{\text{env,obs}} \simeq 2\Gamma_j^2 \delta_p^2 l'^2 U'_j \epsilon c = 3 \times 10^{46} \frac{\Gamma_{j,20}^2 \delta_{p,50}^2 \epsilon_{-1}^3 L_{\text{iso},48}}{\delta_{j,20}^4} \text{ erg/s.} \quad (6)$$

The envelope emission is quite bright. Dividing eqs. (4) and (6), one arrives to a fairly simple expression for the ratio of the plasmoid to envelope luminosities $L_p/L_{\text{env}} \sim 3f_{-1}^2 \delta_{p,50}^2/\Gamma_{j,20}^2 \epsilon_{-1}$. The

timescale (topic of next Section) but is not constraining the fast flares powered by plasmoids.

luminosity contrast depends only on the Lorentz factor of the minijet in the rest frame of the jet $\gamma_p \simeq \delta_p/\Gamma_j$, the size of the plasmoid parametrized by f , and the reconnection rate ϵ . As we discuss in the next Sections, the luminosity ratio is observed to be of order unity constraining $\delta_{p,50}/\Gamma_{j,20} \sim 1$ for $\epsilon \sim f \sim 0.1$. The ratio $\delta_{p,50}/\Gamma_{j,20}$ is determined by the reconnection-induced bulk motions in the jet and points to $\gamma_p \sim 2$ or, equivalently, moderately magnetized jet with $\sigma \sim$ a few.

So far I have considered the emission from a *single* reconnection region which is beaming its emission towards the observer. When the reconnection scale is smaller than the cross section of the jet ($l' < R\theta_j$), there may be as many as $\sim (R\theta_j/l')^3$ reconnection regions in the emitting zone. Even after corrected for beaming of the emission from current sheets, up to $\sim (R\theta_j/l')^3/\gamma_p^2$ reconnection regions may beam their emission towards the observer. The overall amplitude of the envelope emission and the number of fast flares are therefore enhanced by this factor⁷. In this case, the contrast $L_{p,\text{obs}}/L_{\text{env,obs}}$ drops since more than one reconnection layers contribute to the envelope emission.

4 APPLICATION TO OBSERVATIONS

In this section we examine how the wealth of information from fast TeV flaring among blazars can be used to extract information on the physical conditions of the emitting region and constrain the reconnection model. We first discuss observations of several BL Lac objects and then FSRQ PKS 1222.

4.1 Flaring BL Lacs

Fast TeV flares have been observed in several BL Lac objects including PKS 2155, Mrk 501, Mrk 421 and BL Lac itself. The variability timescale ranges from a few to ~ 10 minutes. Most detailed are the observations of PKS 2155 which reveal an envelope emission of duration of hours that contains several ~ 5 -minute flares of comparable luminosity (Aharonian et al. 2007). Mrk 501 also shows flaring with similar flare-to-envelope ratio. BL Lac, the prototype source has also been observed to flare on 10 minutes suggesting that minute-flaring is a generic property of blazars.

Here we apply the model to the, most constraining, PKS 2155 observations (see Aharonian et al. 2007). The observed luminosity of the envelope and of the fast flares is $L_{\text{env}} \sim L_{\text{ff}} \sim 3 \times 10^{46}$ erg/s. The fast flares last for $t_v \sim 5$ min. When the observation started the envelope emission was already on and lasted for ~ 100 min. Narayan & Piran (2012) use Bayesian analysis to estimate the mean duration of the envelope emission of $t_{\text{env}} \sim 2 \times 10^4$ sec. The isotropic equivalent jet power is uncertain but $L_{\text{iso}} \sim 10^{48}$ erg/s appears a reasonable estimate given the *observed* luminosity of the source of up to 10^{47} erg/s and assuming an overall radiative efficiency of 10%. A high Doppler factor $\delta_p \gtrsim 50$ of the emitting material is required for the escape of the TeV radiation from the soft radiation field of the jet without extensive pair creation (Begelman et al. 2008). Observations do not directly constrain where the emission takes place in this source.

The fact that $L_{\text{env}} \sim L_{\text{ff}}$ means that $\gamma_p \sim 2$. Setting $\delta_p = 50$ and $M = 10^9 M_\odot$ and the inferred L_{iso} in eqs. (2), (5), and (6), we derive

⁷ The opposite limit where $l' > R\theta_j$ is not physical since the reconnection region should fit within the jet cross section: the condition $l' \lesssim R\theta_j$ must be satisfied.

all fast flaring and envelope timescales and luminosities in good agreement with the observed values. Moreover, PKS 2155 showed (i) several fast flaring events of (ii) similar characteristic timescale and luminosity. Multiple flares have a natural explanation within the reconnection model. They can be understood to come from different monster plasmoids that emerge from the same reconnection region.

4.2 TeV flares from PKS 1222

The model can also be applied to the FSRQ PKS 1222. In this source the dissipation distance is robustly constrained to be $R_{\text{diss}} \gtrsim 0.5$ pc (Tavecchio et al. 2011; Nalewajko et al. 2012). If the emitting region is characterized by $\delta \sim \Gamma_j \sim 20$ the required luminosity of the jet is unrealistically high (Nalewajko et al. 2012). A moderately higher $\delta \sim 50$ (in agreement to that inferred for PKS 2155) is, however, sufficient to relax the energetic requirements of the jet and is adopted here. Around the epoch of the TeV flare there is an envelope of high γ -ray activity. Fermi-LAT detected a flare of $L_{\text{env}} \sim 10^{48}$ erg/s and duration of roughly $t_{\text{env}} \sim 10^5$ sec (Tanaka et al. 2011; note, however, that *Fermi* observations are not strictly simultaneous with the MAGIC ones). The fast flares are observed with MAGIC in the sub-TeV energy range: $L_{\text{ff}} \sim 10^{47}$ erg/s (with total luminosity possibly higher by \sim a few to account for bolometric corrections in view of the steep observed TeV spectrum). The flux evolved on a timescale of $t_v \sim 7$ min. The isotropic equivalent jet power is also uncertain but $L_{\text{iso}} \sim 10^{49}$ erg/s appears a reasonable estimate given that the observed disk emission is several 10^{46} erg/s and that the beamed observed radiative luminosity of the jet reaches 10^{48} erg/s.

Setting $\delta_p = 50$, $L_{\text{iso}} \sim 10^{49}$ erg/s, one can verify that the observed duration of the envelope and of the fast flare are reproduced by the model. The same holds true for the flare luminosity. The observed envelope emission is observed to be more luminous than the fast flare by a factor of several (though weaker, the fast flare is clearly observed with MAGIC because of its harder emission). Given the adopted parameters, eq. (4) implies that a single reconnection region has envelope luminosity $L_{\text{env}} \sim L_{\text{ff}}$ while the envelope was a factor of \sim several brighter in this source. Possibly several reconnection layers contribute to the envelope emission simultaneously if $R\theta_j/l' \sim$ several, enhancing the ratio of the luminosity of the envelope emission with respect to that of fast flares.

Summarizing all blazar flares can be accounted for by little changes of the physical parameters of the model. Typically I infer $\Gamma_j \sim 20$, $\gamma_p \sim 2$ and the size of the reconnection region $l' \lesssim 10^{16}$ cm. The blazar zone is located at $R_{\text{diss}} \sim (0.3 - 1)$ pc.

4.3 Radiative mechanisms and particle cooling

The energetic requirements for the fast flaring can become more stringent if the radiating particles (assumed to be electrons) are not in the fast cooling regime. Here we assume that the TeV emission is either result of synchrotron self Compton (SSC) or external inverse Compton (EIC) and investigate the electron energetics required to produce the observed ~ 100 GeV- multi TeV emission and whether they are likely to radiate efficiently for the model parameters adopted in the previous Section. In the end of the Section, I discuss the expectation of X-ray flares as result of synchrotron radiation from the same population of electrons.

To assess whether the emitting particles “cool fast”, the expansion timescale of the plasmoid $t''_{\text{exp}} = R''/c = \delta_p t_v = 3 \times 10^4 \delta_{50} t_{v,10}$

is to be compared with the radiative cooling timescale. In the case of SSC emission from e^- (or pairs) with random Lorentz factor γ_e in magnetic field B'' , the characteristic energy is $e_{\text{SSC}} \approx 10^{-8} \delta_p \gamma_e^4 B''$ eV. Depending on details of the reconnection configuration (such as guide field strength), the plasmoid can be magnetically or heat dominated⁸. For simplicity, I parametrize the magnetic field strength in the plasmoid as $B'' = (\epsilon_B 4\pi U_p'')^{1/2} = 0.7 \epsilon_{B,1/3}^{1/2} L_{\text{iso},48}^{1/2} \epsilon_{-1} M_9^{-1} \Gamma_{j,20}^{-1} \delta_{j,20}^{-2}$ Gauss. Setting $e_{\text{SSC}} = 100 e_{100\text{GeV}}$ GeV, one finds for the required electron (random) Lorentz factor $\gamma_e = 2 \times 10^4 e_{100\text{GeV}}^{1/4} M_9^{1/4} \Gamma_{j,20}^{1/4} \delta_{j,20}^{1/2} \epsilon_{-1}^{-1/4} \epsilon_{B,1/3}^{-1/8} L_{\text{iso},48}^{-1/8} \delta_{p,50}^{-1/4}$. The SSC cooling time scale is $t''_{\text{SSC}} = 5 \times 10^8 / (1 + y) \gamma_e B''^2$ s or

$$t''_{\text{SSC}} \approx 1.5 \times 10^4 \frac{3}{1 + y} \frac{\delta_{p,50}^{1/4} M_9^{7/4} \Gamma_{j,20}^{7/4} \delta_{j,20}^{7/2}}{e_{100\text{GeV}}^{1/4} \epsilon_{-1}^{7/4} \epsilon_{B,1/3}^{7/8} L_{\text{iso},48}^{7/8}} \text{ s}, \quad (7)$$

where $y \sim$ a few accounts for the ratio of the SSC to synchrotron power.

If a substantial external radiation field of energy density U_{rad} is present, it can contribute to the particle cooling through EIC. Assuming an isotropic radiation field of characteristic energy e_{seed} , the energy of the up-scattered photon is $e_{\text{EIC}} \approx \Gamma_p \delta_p \gamma_e^2 e_{\text{seed}}$ (for scattering in the Thomson limit). Solving for the electron Lorentz factor: $\gamma_e \approx 7 \times 10^3 (e_{\text{EIC},100\text{GeV}}/e_{\text{seed},1})^{1/2} \delta_{50}^{-1}$, where $e_{\text{seed},1}$ eV and $\Gamma_p \approx \delta_p$. The energy density of radiation in the rest frame of the blob is $U''_{\text{rad}} \approx \Gamma_p^2 U_{\text{rad}}$. The EIC cooling timescale for such electron is $t''_{\text{EIC}} = 2 \times 10^7 / \gamma_e U''_{\text{rad}}$ s or

$$t''_{\text{EIC}} = \frac{1.4 \times 10^4}{U_{\text{seed},-4} \delta_{p,50}} \left(\frac{e_{\text{seed},1}}{e_{100\text{GeV}}} \right)^{1/2} \text{ s}, \quad (8)$$

for $U_{\text{seed}} = 10^{-4} U_{\text{seed},-4}$ erg cm⁻³.

In the case of PKS 2155 no powerful ambient isotropic radiation field is evident. The plasmoid may well propagate into a dense radiation field emerging from the large scale jet or other reconnection regions. This depends however on uncertain details of the overall geometry (see Nalewajko et al. 2011 for various possible geometrical configurations). On the other hand SSC emission has to be present. Setting the model parameters to those relevant for PKS 2155 (see previous Section), and $\epsilon_B = 1/3$, $y = 2$, I arrive at $t_{\text{SSC}} \lesssim 10^4$ s (see eq. 5). This timescale is, by a modest factor, shorter than the expansion time of the blob $t''_{\text{exp}} = 1.5 \times 10^4 \delta_{50} t_{v,5}$ s indicating that efficient \sim TeV emission is plausible. The required random Lorentz factor of the emitting electrons is $\gamma_e \gtrsim 10^4$.

One can derive a similar estimate for the SSC cooling timescale for the parameters relevant to PKS 1222 flaring, i.e. $t''_{\text{SSC}} \lesssim t''_{\text{exp}} \sim 2 \times 10^4$ s. Another obvious possibility for emission from this source is EIC of photons from the infrared torus. With $U_{\text{IR}} \sim 10^{-4}$ erg cm⁻³ and characteristic energy $e_{\text{IR}} \sim 0.3$ eV, the EIC takes place in the Thomson regime (Nalewajko et al. 2012). The typical electron emitting ~ 100 GeV has $\gamma_e \sim 10^4$ with a cooling time scale of the particles of $t''_{\text{EIC}} \sim 8 \times 10^3$ s $\sim t''_{\text{SSC}} \lesssim t''_{\text{exp}}$.

In Summary the \sim TeV emitting electrons are characterized by a random $\gamma_e \sim 10^4$ and have a cooling timescale somewhat shorter than the expansion timescale of the blob allowing for efficient TeV emission. The detailed spectrum necessarily depends on the details of the particle distribution that are model dependent. However, an equipartition argument (e.g. sharing of the dissipated magnetic energy between electrons and protons) would give

⁸ The fact that the jet is Poynting-flux dominated in this model does not necessarily mean that the emitting region is also strongly magnetized. On the contrary, efficient reconnection may result in weakly-magnetized (heat-dominated) plasmoids.

$\gamma_e \sim (m_p/2m_e)\sigma \simeq 3 \times 10^3 \sigma_3$ for the electrons in the plasmoid, where $\sigma = 3\sigma_3$ is the upstream magnetization. Therefore, a modest particle acceleration above equipartition is sufficient to explain the observed emission.

For the typical conditions inferred in the emitting region ($\gamma_e \gtrsim 10^4$, $B'' \sim 1$ Gauss, $\delta_p \sim 50$), the synchrotron component naturally peaks in the soft X-ray band. If SSC is the mechanism for the very high energy emission, the synchrotron component may be quite powerful $L_{\text{syn}} = L_\gamma/y$. Fast X-ray flares, simultaneous to the very-high energy ones, are therefore quite likely in this model (see the Discussion section for observational evidence for such flaring).

5 DISCUSSION/CONCLUSIONS

The similarities in the variability patterns in several blazars (PKS 1221, PKS 2155, BL Lac, Mrk 501) are striking: fast TeV flares on \sim minutes timescale that appear on top of an envelope of enhanced gamma-ray activity that lasts for hours or days. The similarities strongly indicate similar physical conditions at the emitting region: large Doppler factor $\delta_p \sim 50$ and a dissipation zone located at \sim pc distance from the black hole.

5.1 Models for fast blazar flaring

Several suggestions have been put forward for the ultrafast blazar flaring. Fast electron beams (with bulk $\gamma_e \sim 10^6$) may develop along magnetic field lines close to the light cylinder (i.e. within several R_{Sch} , see, Ghisellini & Tavecchio 2008). The TeV flare, in this scenario, is result of the beam inverse Compton scattering external radiation fields. This model fails to account for the large emission distance required by PKS 1222 (Aleksić et al. 2011). For a hadronic model applicable to the fast flares of PKS 1222 see Dermer et al. (2012). In this model $\gtrsim 100$ TeV neutrinos are predicted. Alternatively, a red giant may cross the jet (Barkov et al. 2012). The ram pressure of the jet strips the envelope of the star which consequently fragments. Emission from shocked stellar and/or jet plasma may power blazar flares. While stellar-jet encounters are expected, any interaction region will necessarily move slower than the jet $\Gamma_{\text{int}} \lesssim \Gamma_j$. The required Doppler boost of the emitting region towards the observer $\delta \sim 50$ may therefore be hard to explain in this picture. Alternatively, a recollimation shock on pc scales can help to focus the jet energy in a small region inducing short timescale viability. However, non-axisymmetries in the jet-external medium interaction will likely make the focusing insufficient to explain the most extreme flares (Bromberg & Levinson 2009). If the jet activity is sufficiently erratic, the jet can be envisioned as magnetized shells separated by vacuum (Lyutikov & Lister 2010). Rarefaction waves of the front part of a shell can reach a bulk Lorentz factor much higher than that of the jet on average. Fast flares may come from these rarefied regions. Relativistic turbulence in the jet can also allow for emitters-blobs moving with $\Gamma_b \gg \Gamma_j$ to be responsible for intense and fast flares (Narayan & Piran 2012). For the turbulence not to be supersonic (or it would decay fast by shocks) the jet must be Poynting flux dominated. The driver and the region where the turbulence develops remain to be identified. Magnetic reconnection could drive the turbulent motions (and turbulence can, in turn, enhance the reconnection rate; Lazarian & Vishniac 1999). In this case, however, it is quite likely that the most powerful flares are directly related to the driver, i.e., the reconnection process itself rather than the turbulent motions.

5.2 The reconnection model for fast flaring

Here we have revisited the reconnection minijet model for the fast flaring (Giannios et al. 2009; 2010). We focus on time-dependent aspects that are naturally expected (and directly observed in laboratory experiments and solar system environment) in the reconnection process. It is demonstrated that at least two timescales appear in the problem. The longer one is associated with the time it takes for a magnetic energy to be dissipated in the reconnection region and creates an “envelope” of flaring activity that lasts for several hours to days. Instabilities in the current sheet (e.g. secondary tearing instability; Loureiro et al. 2007) result in erratic formation of plasmoids that leave the reconnection region at relativistic speed. The largest ones, “monster” plasmoids, can power the fast, $\lesssim 10$ minute-long blazar flares. Several to tens of monster plasmoids can emerge from a single reconnection layer. The super-fast flaring may therefore not happen in isolation. *A sequence of fast flares are expected to have similar timescale set by the size of the reconnection layer as observed in PKS 2155.* Verification of this trend of a sequence of flares in more sources and/or in other bands such as X-rays (see below) would provide strong support for the model.

A virtue of the model is that it can be applied to all blazar sources with observed fast flaring for similar adopted parameters. In this model, the dissipation of energy that powers the blazar radiation takes place at distance $R_{\text{diss}} \sim 0.3 - 1$ pc, the bulk Lorentz factor of the jet is $\Gamma_j \sim 20$, and the size of the reconnection region $l' \lesssim 10^{16}$ cm. These quantities point towards an interesting possibility for the magnetic field structure in the jet and the origin of the blazar emission. If the magnetic field configuration is not exactly axisymmetric at the horizon, the jet may emerge with small-scale field structures of size similar to that of the central engine $\sim R_{\text{Sch}} \sim 3 \times 10^{14} M_9$ cm (along the direction of the jet propagation). Even a modest non-axisymmetry at the base of the jet can be amplified by stretching in the toroidal direction because of the jet (lateral) expansion. The jet expands from a lateral size of $r \sim R_{\text{Sch}}$ at the launching radius to $r = \theta_j R_{\text{diss}} \gg R_{\text{Sch}}$ at the dissipation distance. The resulting scale of the field reversals in the rest frame of the jet is $\sim \Gamma_j R_{\text{Sch}}$ that may be used as an estimate of the characteristic scale of the reconnection layer $l' \lesssim 10^{16}$ cm. For typical parameters, the reconnection time catches up with the expansion time of the jet at distance $R_{\text{diss}} \sim \Gamma_j^2 R_{\text{Sch}} / \epsilon \sim 1$ pc.

The very-high energy flares are modeled to be result of SSC or EIC process of energetic electrons in the plasmoids, depending on the source. For the physical parameters inferred at the emitting region, however, the synchrotron emission from the same population of electrons naturally peaks in the X-ray band. In, at least some, of the sources fast γ -ray flares should also be accompanied by fast X-ray flaring. Evidence for ultra-fast flares has existed for some time. For instance Cui (2004) shows, using *RXTE* observations of Mrk 421, that X-ray flaring on timescales as short as ~ 10 minutes is evident. Also, a characteristic envelope-fast flares structure is evident (see their Fig. 10). Simultaneous detection of fast flares in both X-ray and γ -ray bands will be very informative and constraining for the models.

The bulk motion of plasmoids in the jet rest frame required for the model to work are very modest $\gamma_p \sim 2$. The bulk motion in the reconnection picture corresponds to the Alfvén speed: $\gamma_p \simeq \sqrt{1 + \sigma}$, implying that a magnetization $\sigma \sim 3$ is required at the dissipation zone R_{diss} . Is it reasonable that the jet remains modestly Poynting-flux dominated at ~ 1 pc scale? This would imply that the conversion of Poynting-to-kinetic flux is not complete by

that distance. A systematic study of superluminal motions on pc to tens of pc scales reveals that blazar jets still undergo acceleration out to the larger scale (Piner et al. 2012). In the context of MHD acceleration of jets, this would imply that, indeed, the pc-scale jet maintains a substantial magnetization.

Ultra-fast flares are the tip of the iceberg of blazar variability. The process of magnetic reconnection is potentially responsible for powering a much broader range of blazar activity. Reconnection may well take place at larger (e.g. multi pc) scale where the plasma is presumably less magnetized (because of further conversion of magnetic energy into kinetic). When the reconnecting plasma is characterized by $\sigma \lesssim 1$, the reconnection speed v_{rec} slows down (since $v_{\text{rec}} \propto V_A < c$). In this case, the reconnection timescale becomes longer and reconnection layers may power days-to-weeks long flares of “envelope” emission.

5.2.1 Other Astrophysical implications

These ideas of plasmoid-dominated reconnection may be applied to other Astrophysical sources. The variability patterns of gamma-ray burst (GRB) emission show fast flaring on top of slower-evolving lightcurves that may be connected to such reconnection process (see also Lyutikov 2006; Lazar et al. 2009; McKinney & Uzdensky 2012; Zhang & Yan 2011). Similar considerations may apply to flares observed during the GRB afterglows (Giannios 2006). Reconnection minijets may also be the key to understand the fast GeV flaring of the pulsar wind nebula of Crab (Clausen-Brown & Lyutikov 2012; Cerutti et al. 2012). In particular such model can attempt to explain the day-long flares and shorter timescale variability observed during major flaring of the Crab (Abdo et al. 2011; Tavani et al. 2011; Buehler et al. 2012).

5.2.2 Open issues

This study focused on the rough energetics and timescales of plasmoid-dominated reconnection in blazar jets. While the feasibility of the process to account for blazar flares has been made, a more detailed comparison to observations requires progress in our theoretical understanding on a number of fronts.

Where is the dissipation zone of jets located? Studies of the global jet structure and stability can reveal where and why reconnection in the jet develops. These studies will also probe the characteristic length scales and orientation of the reconnection regions. The plasmoid-dominated reconnection is also a study in progress. Better understanding of fragmentation instabilities of the current sheet requires high-resolution 3D simulations. The theory should be tested and extended to the, interesting here, trans-relativistic $\sigma \sim$ a few regime. Finally for making predictions on the spectra of the resulting emission and direct comparison to observations, a better understanding of particle acceleration in reconnection regions is required. Particle-in-cell simulations make rapid progress in this direction (Zenitani & Hoshino 2005; Drake et al. 2006; Sironi & Spitkovsky 2011).

ACKNOWLEDGMENTS

I thank H. Spruit and D. Uzdensky for insightful discussions and comments during the preparation of the manuscript. I thank the referee for carefully reading the manuscript, spotting inaccuracies in the derivations and making suggestions that greatly improved the manuscript.

REFERENCES

- Abdo A. A., Ackermann M., Ajello M., et al., 2011, *Science*, 331, 739
- Aharonian F., Akhperjanian A. G., Bazer-Bachi A. R., et al., 2007, *ApJ*, 664, L71
- Arlen T., Aune, T., Beilicke, M., et al., 2013, *ApJ*, 762, 92
- Albert J. et al., 2007, *ApJ*, 669, 862
- Aleksić J., Antonelli L. A., Antoranz P., et al., 2011, *ApJ*, 730, L8
- Aschwanden M. J., 2002, *Space Science Reviews*, 101, 1
- Barkov M. V., Aharonian F. A., Bogovalov S. V., Kelner S. R., Khangulyan D., 2012, *ApJ*, 749, 119
- Begelman M. C., 1998, *ApJ*, 493, 291
- Begelman M. C., Fabian A. C., Rees M. J., 2008, *MNRAS*, 384, L19
- Bhattacharjee A., Huang Y.-M., Yang H., Rogers B., 2009, *Physics of Plasmas*, 16, 112102
- Blandford R. D., Payne D. G., 1982, *MNRAS*, 199, 883
- Böttcher M., 2007, *Ap&SS*, 309, 95
- Bromberg O., Levinson A., 2009, *A&A*, 699, 1274
- Buehler R., Scargle J. D., Blandford R. D., et al., 2012, *ApJ*, 749, 26
- Cerutti B., Werner G. R., Uzdensky D. A., Begelman M. C., 2012, *ApJ*, 754, L33
- Clausen-Brown E., Lyutikov M., 2012, *MNRAS*, 426, 1374
- Cui W. 2004, *ApJ*, 605, 662
- Daughton W., Roytershteyn V., Albright B. J., et al., 2009, *Phys. Rev. Letters*, 103, 065004
- Dermer C. D., Murase K., Takami H. 2012, *ApJ*, 755, 147
- Drake J. F., Swisdak M., Che H., Shay M. A., 2006, *Nature*, 443, 553
- Eichler D., 1993, *ApJ*, 419, 111
- Finke J. D., Dermer C. D., Böttcher M., 2008, *ApJ*, 686, 181
- Gaidos J. A., Akerlof C. W., Biller S., et al., 1996, *Nature*, 383, 319
- Giannios D., 2006, *A&A*, 455, L5
- Giannios D., 2010, *MNRAS*, 408, L46
- Giannios D., Spruit H. C., 2006, *A&A*, 450, 887
- Giannios D., Uzdensky D. A., Begelman M. C., 2009, *MNRAS*, 395, L29
- Giannios D., Uzdensky D. A., Begelman M. C., 2010, *MNRAS*, 402, 1649
- Ghisellini G., Tavecchio, F., 2008, *MNRAS*, 386, L28
- Goodman J., Uzdensky D., 2008, *ApJ*, 688, 555
- Karlický M., Kliem B., 2010, *Solar Physics*, 266, 71
- Kulsrud R. M., 2001, *Earth, Planets, and Space*, 53, 417
- Lapenta G., 2008, *Phys. Rev. L*, 100, 235001
- Lazar A., Nakar E., Piran T., 2009, *ApJ*, 695, L10
- Lazarian A., Vishniac E. T., 1999, *ApJ*, 517, 700
- Levinson A., van Putten M. H. P. M., 1997, *ApJ*, 488, 69
- Lin J., Ko Y.-K., Sui L., et al., 2005, *ApJ*, 622, 1251
- Loureiro N. F., Schekochihin A. A., Cowley, S. C. 2007, *Physics of Plasmas*, 14, 100703
- Loureiro N. F., Uzdensky D. A., Schekochihin A. A., Cowley S. C., Yousef T. A., 2009, *MNRAS*, 399, L146
- Loureiro N. F., Samtaney R., Schekochihin A. A., Uzdensky D. A., 2012, *Physics of Plasmas*, 19, 042303
- Loureiro N. F., Schekochihin A. A., Uzdensky D. A., 2013, *Phys. Rev. E*, 87, 013102
- Lyubarsky Y. E., 2005, *MNRAS*, 358, 113
- Lyutikov M., 2006, *New Journal of Physics*, 8, 119
- Lyutikov M., Lister M., 2010, *ApJ*, 722, 197

Mastichiadis A., Moraitis K. 2008, A&A, 491, L37
 Malyshkin L. M., 2008, Phys. Rev. L, 101, 225001
 McKinney J. C., Uzdensky D. A., 2012, MNRAS, 419, 573
 Moll R., 2009, A&A, 507, 1203
 Nalewajko K., Giannios D., Begelman M. C., Uzdensky D. A., Sikora M., 2011, MNRAS, 413, 333
 Nalewajko K., Begelman M. C., Cerutti B., Uzdensky D. A., Sikora M., 2012, MNRAS, 425, 2519
 Narayan R., Piran T., 2012, MNRAS, 420, 604
 Park H. K., Luhmann N. C. Jr., Donn e A. J. H., et al., 2006, Phys. Rev. L, 96, 195003
 Parker E. N. 1957, Journal of Geophysical Research, 62, 509
 Petschek H. E., 1964, The Physics of Solar Flares, 425
 Piner B. G., Pushkarev A. B., Kovalev Y. Y., et al., 2012, ApJ, 758, 84
 Pushkarev A. B., Kovalev Y. Y., Lister M. L., Savolainen T., 2009, A&A, 507, L33
 Romanova M. M., Lovelace R. V. E., 1997, ApJ, 475, 97
 Samtaney R., Loureiro N. F., Uzdensky D. A., Schekochihin A. A., Cowley S. C., 2009, Phys. Rev. L, 103, 105004
 Savolainen T., Homan D. C., Hovatta T., et al., 2010, A&A, 512, A24
 Sironi L., Spitkovsky A., 2011, ApJ, 741, 39
 Sweet P. A. 1958, Electromagnetic Phenomena in Cosmical Physics, 6, 123
 Tanaka Y. T., Stawarz Ł., Thompson D. J., et al., 2011, ApJ, 733, 19
 Tavani M., Bulgarelli A., Vittorini V., et al., 2011, Science, 331, 736
 Tavecchio F., Ghisellini G., 2012, MNRAS, submitted
 Tavecchio F., Becerra-Gonzalez J., Ghisellini G., et al., 2011, A&A, 534, A86
 Urry C. M., Padovani P., 1995, Publications of the Astronomical Society of the Pacific, 107, 803
 Uzdensky D. A., Loureiro N. F., Schekochihin A. A., 2010, Phys. Rev. L, 105, 235002
 Zenitani S., Hoshino M., 2001, ApJ, 562, L63
 Zenitani S., Hoshino M., 2005, ApJ, 618, L111
 Zhang B., Yan H., 2011, ApJ, 726, 90

$\eta_c \sim 10^5 \text{ cm}^2/\text{s}$. The Lundquist number is $S \sim 10^{21}$ clearly far in excess the critical value $S_c \simeq 10^4$ above which the secondary tearing instability in the current sheet sets in (and $S \gg 10^5$ as required for monster plasmoids to develop). Reconnection in blazars is, therefore, likely to take place in the plasmoid-dominated regime.

As discussed in Uzdensky et al. (2010) the plasmoids have a hierarchical structure with a large range in size. Large plasmoids are separated by a secondary reconnection layer of length $l^{(2)}$ where, in turn, smaller plasmoids form. This hierarchy repeats on ever smaller scales $l^{(n)}$. The smallest structure would formally be a ‘‘critical layer’’ of length $l_c = S_c \eta / c \sim 1 \text{ mm}$ with nominal thickness $\delta_c = S_c^{-1/2} l_c \sim 10^{-3} \text{ cm}$! Such small structures are never realized in practice because the characteristic plasma scales (e.g. the ion skin depth d_i) are much larger. For the expected plasma density of the jet $d_i \sim 10^8 \text{ cm}$. Once the thickness of a sublayer $\delta \sim d_i$, the resistive MHD description fails. One instead deals with ‘‘collisionless’’ reconnection where the resistivity is likely to be controlled by plasma instabilities. In this regime, the Petschek model for (relativistic) reconnection (Lyubarsky 2005) may apply (Kulsrud 2001). The Petschek reconnection rate at a layer of length $l = S_c^{1/2} d_i \sim 10^{10} \text{ cm}$ is $v_{\text{rec}} \sim c / \ln S_p \sim 0.03c$, where $S_p = lc/\eta \sim 10^{15}$. Moreover, when $\delta \sim d_i$, Hall MHD terms become important further increasing the reconnection rate (see, e.g., Malyshkin 2008). This local fast reconnection rate controls also the overall rate of large-scale reconnection (Uzdensky et al. 2010).

APPENDIX A: PROPERTIES OF THE RECONNECTION REGION IN BLAZARS

Here I estimate the Lundquist number $S = l' V_A / \eta$ that characterizes the reconnection region in a blazar jet as well as several physical scales of relevance to the structure of the current sheet. I focus on modestly high- σ upstream (i.e., $\sigma \sim$ a few). The resulting Alfv en speed $V_A = \sqrt{\sigma/(1+\sigma)}c \simeq c$. The size of the reconnection region is constrained from the observed duration of the blazar flares to $l' \lesssim 10^{16} \text{ cm}$.

The resistivity η contains contributions from Coulomb collisions η_s (Spitzer resistivity) and electron scattering by photons η_c (the, so called, ‘‘Compton drag’’; Goodman & Uzdensky 2008). For any reasonable temperature of the electrons in the jet, the Compton drag is expected to dominate over the Spitzer resistivity. Following Goodman & Uzdensky (2008) $\eta_c = c\sigma_T U'_{\text{rad}} / 3\pi e^2 n_e$. For the very rough, order-of-magnitude estimate performed here we can set $U'_{\text{rad}} \sim U'_j$ (i.e., much of the energy density of the jet - as given in eq. (1) - converts to radiation) and $n_e = n_p = U'_j / (1 + \sigma) m_p c^2$ for an electron-proton jet. For $R_{\text{diss}} \sim 1 \text{ pc}$ the resulting resistivity